

## Article

# Impact of Solar Radiation on Luminaires and Energy Efficiency in Isolated Residential Photovoltaic Systems

Jaime Jalomo-Cuevas <sup>1</sup>, Fabiola Colmenero Fonseca <sup>2,\*</sup>, Javier Cárcel-Carrasco <sup>2</sup>, Sergio Sandoval Pérez <sup>1</sup>  
and Alberto Gudiño-Ochoa <sup>1</sup>

<sup>1</sup> Electronics Department, Tecnológico Nacional de México/Instituto Tecnológico de Ciudad Guzmán, Ciudad Guzmán 49100, Mexico; jaime.jc@cdguzman.tecnm.mx (J.J.-C.); sergio.sp@cdguzman.tecnm.mx (S.S.P.); m21290934@cdguzman.tecnm.mx (A.G.-O.)

<sup>2</sup> Institute of Materials Technology, Universitat Politècnica de València, 46022 Valencia, Spain; fracarc1@csa.upv.es

\* Correspondence: fcolfon@upvnet.upv.es

**Abstract:** This research centers on the implementation of photovoltaic systems in residential applications, coupled with battery-based energy storage, and evaluates their efficiency in generating energy, specifically for lighting in buildings. The methodology hinges on detecting interharmonic signals to characterize potentially disruptive frequencies and identify the origins of various failures. Multiple case studies are presented to validate the method's efficacy, including one involving fluorescent lamp circuits and another examining variations in solar radiation during the summer season. Real-world experiments are conducted in a residential setting, and the results are thoroughly analyzed. Various types of interharmonic generation behaviors are demonstrated, which are influenced by fluctuations in solar radiation and the appropriate installation of solar panels. The findings reveal that the absence of solar radiation below 300 W/m<sup>2</sup> in a photovoltaic system relying on energy storage adversely affects interharmonics in luminaires installed within a residential space.

**Keywords:** solar energy; photovoltaic systems; interharmonics; luminaries



Citation: Jalomo-Cuevas, J.;

Colmenero Fonseca, F.;

Cárcel-Carrasco, J.; Pérez, S.S.;

Gudiño-Ochoa, A. Impact of Solar Radiation on Luminaires and Energy Efficiency in Isolated Residential Photovoltaic Systems. *Buildings* **2023**, *13*, 2655. <https://doi.org/10.3390/buildings13102655>

Received: 16 September 2023

Revised: 9 October 2023

Accepted: 18 October 2023

Published: 21 October 2023



**Copyright:** © 2023 by the authors. Licensee MDPI, Basel, Switzerland. This article is an open access article distributed under the terms and conditions of the Creative Commons Attribution (CC BY) license (<https://creativecommons.org/licenses/by/4.0/>).

## 1. Introduction

At present, global population growth has surged disproportionately, leading to heightened demands for resources across various facets of our planet [1]. In response to the interplay of population growth and environmental concerns, the United Nations has outlined 17 Sustainable Development Goals (SDGs) within the 2030 Agenda, aimed at addressing both environmental and population-related challenges. This study focuses on the seventh SDG, which emphasizes the promotion of clean energy sources, their productivity, and quality [2]. Specifically, it advocates for ‘*Expanding infrastructure and upgrading technology for clean energy in all developing countries*’, recognizing the pivotal role it plays in fostering growth while also benefiting the environment. The utilization of solar energy aligns with the concept of zero-energy buildings and holds significant potential for mitigating climate change. Zero-energy buildings are a pivotal component of future city decarbonization efforts [3,4]. Moreover, the deployment of residential solar systems has demonstrated economic viability, particularly for microenterprises and low-income households engaged in various income-generating activities, extending beyond just lighting purposes [5].

Photovoltaic technology has made a significant global impact, particularly in large buildings, where it has enhanced indoor natural lighting efficiency, boosted performance in outdoor lighting system designs, and heightened overall security [6]. Many governments worldwide have adopted sustainable city goals as a response to issues such as overpopulation, pollution, and global warming [7]. In tropical regions, innovative technology applications demonstrate how suburban buildings can benefit from attached greenhouses,

which help regulate indoor temperatures and generate energy for household consumption [8]. Multi-family residential buildings that incorporate solar systems yield greater amounts of both electrical and thermal energy compared to conventional systems within the same multifamily building installation, playing a crucial role in the decarbonization effort [9].

The economic viability of harnessing solar energy for various residential applications is evident, considering both the technical aspects of solar panel installation and their financial advantages. This encompasses panel orientation and optimal angles based on the architectural characteristics of the residence [10]. Additionally, photovoltaic semitransparent panels can be employed as building facades to efficiently control indoor climate, as roof-installed panels alone may not suffice to reduce indoor temperatures or supply a significant portion of the energy consumed by building occupants [11]. However, it is important to note that the temperature differential depends on factors such as time of day and season, influenced by both external and internal conditions [12]. Therefore, it is crucial to consider the environmental factors related to solar radiation and local climate, emphasizing the promotion of energy-efficient buildings and residences with a focus on achieving zero-energy status. It is worth noting that, due to anticipated changes in climate conditions in the coming years, solar radiation is expected to increase by 4.7% [13].

In light of this context, concurrent Architectural Photovoltaic Applications (APA) should be integrated into the design concept and process, resulting in substantial integration [14]. During the winter months, solar radiation may not be sufficient for energy conversion in a photovoltaic system designed for residential use. Consequently, under such conditions, the solar energy supply during the day may meet energy demands for this time of year with appropriate system installation considerations [15]. Designing photovoltaic systems integrated into buildings involves the use of relevant renewable energy sources while also considering energy-efficient arrangements [16]. Assuming these conditions, it has been observed that solar irradiance influences facades with photovoltaic systems, with diffuse solar radiation contributing significantly to the overall solar radiation. These factors notably impact the energy performance indicators of residential buildings [17]. Even in residences where an isolated photovoltaic system is proposed, relying on battery storage, variations in predicted solar radiation and battery degradation are dependent on the total energy consumption of appliances, revealing a correlation between solar radiation and the capabilities of the photovoltaic battery system [18]. Similarly, in multi-generational energy systems based on solar energy for residential houses, there is a linear increase in energy production with the improvement of panel efficiency and solar irradiation [19].

Recent years have witnessed the study of the interharmonic phenomenon due to the expansion of the electric grid and the integration of complex nonlinear loads such as fluorescent lamps and frequency converters for both home and industrial use [20]. The impact of harmonics on the grid and electrical and electronic equipment necessitates examination to mitigate significant issues, including high-cost repairs, reductions in useful lifetime, equipment overheating, acoustic disturbances, and mechanical system oscillations. Globally, the cost of replacing or repairing damaged technology continues to rise each year, exacerbated by the growing issue of electronic waste, which is closely tied to global warming [21,22].

Photovoltaic technology and interharmonics are closely intertwined due to the use of converters and maximum power point tracking (MPPT) controllers, as well as environmental conditions, particularly solar irradiance. Interharmonics introduce non-multiple-frequency distortions in current or voltage, thereby limiting power quality (PQ) and affecting electrical grids [23,24]. Recent studies have examined the impact of interharmonics, with a focus on their association with electric loads operating under non-steady-state conditions, non-linear loads, double AC/DC/AC and DC/AC energy conversion systems, and photovoltaic systems as renewable energy sources [25–28]. The Flicker effect, another adverse influence on electrical grids, is perceptible as visible fluctuations in the intensity of light from fluorescent and LED lamps, caused by transient voltage changes, and is related

to harmonics and interharmonics [20,29,30]. Furthermore, interharmonics can affect the lifespan of critical components for reliability, such as power converters and batteries, thus necessitating their consideration in economic assessments [31].

Considering the generation of interharmonics in photovoltaic systems geared towards energy efficiency and their strong dependence on environmental factors, as well as their economic benefits in isolated networks with domestic energy storage, which prove more cost-effective [32] and contribute to reduced CO<sub>2</sub> emissions, it becomes evident that assessing their impact on power quality and issues related to harmonic and interharmonic generation in photovoltaic systems, especially those affecting luminaires in residential spaces, is of paramount importance. The evaluation of the reliability of energy conversion units (representing the most critical components for system reliability) [33,34], including the performance and lifespan of devices involved in the photovoltaic system due to solar radiation and ambient temperature under different configurations, becomes crucial. Variations that alter the tilt and orientation of photovoltaic panels impact the system's lifespan and depend on its location [24,35,36].

The primary focus of this study underscores the presence and significance of interharmonic generation in an isolated photovoltaic system, primarily designed for fluorescent lighting installation in a residential setting under varying solar irradiance conditions. Beyond its implications for energy system efficiency, it can even affect certain interconnected electronic and domestic equipment within the photovoltaic system. We present evidence of non-linear loads such as fluorescent lamps, where the most detrimental and pronounced effects occur during the switching of ON/OFF under different solar irradiance conditions, affecting the system, especially under partial solar irradiance. Electrical measurements of current and voltage in the luminaires are analyzed using time-frequency analysis with spectrograms. A second experiment is conducted, introducing changes in sunlight intensity by partially shading the photovoltaic panels to prevent direct sunlight from reaching the silicon surface, where transients produce interharmonic patterns. The experiments were conducted on a real platform equipped with photovoltaic panels connected in series, an MPPT charge controller, a DC/AC converter, and fluorescent lamps. Load levels and voltage were calculated to meet the lighting needs of a standard household accommodating a family of four.

## 2. Materials and Methods

To understand the performance of the PV system, analyses that include solar radiation as part of PV power generation specifications must be performed.

### 2.1. Modeling of the Sun Position

The determination of an observer at a specific point on Earth and the position of the sun are obtained by two main angles: the altitude angle  $\alpha$  (°) and the azimuth angle  $\theta_s$  (°). The altitude angle, or solar zenith angle, corresponds to the angular height of the sun in the sky measured from the horizontal [37]:

$$\sin \alpha = \sin \mathcal{L} \sin \delta + \cos \mathcal{L} \cos \delta \cos \omega \quad (1)$$

where  $\mathcal{L}$  is the latitude of the location,  $\delta$  is the angle of declination, and  $\omega$  is the hour angle. Therefore, the azimuth angle refers to the angular displacement of the sun's reference line from the source axis. Figure 1 illustrates the positioning of the solar panel, facing south, along with its inclination angle  $\beta$  (°). This configuration considers the sun's path as the reference, as well as the relevant angles, including the altitude and azimuth angles. The azimuth angle is given by [38]:

$$\sin \theta = \frac{\cos \delta \sin \omega}{\cos \alpha} \quad (2)$$

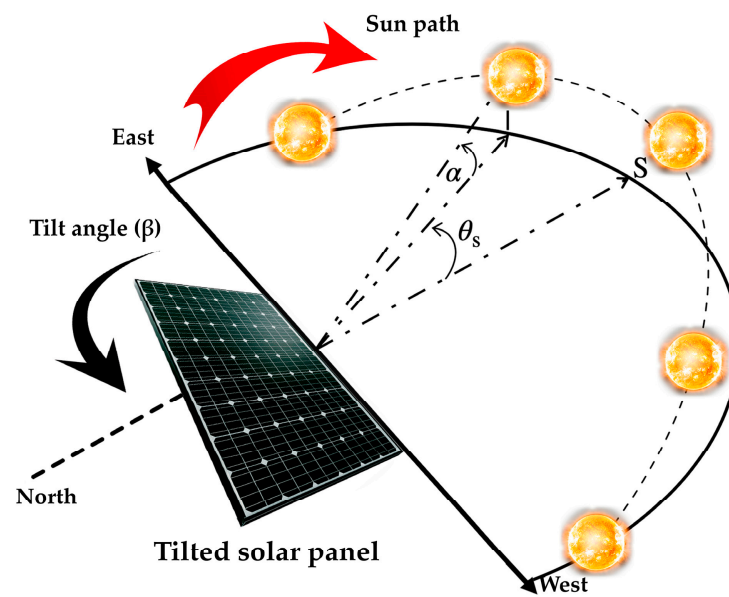


**Figure 1.** Sun's altitude and azimuth angles.

## 2.2. Modeling of Extraterrestrial Solar Radiation

The spectral distribution of the radiation emitted from the surface of the sun in relation to the prediction of Planck's theorem [39] is equal to  $1367 \text{ W/m}^2$  of solar radiation outside the earth's atmosphere, called the solar constant  $G_{sc}$ . The direct radiation of the plane normal to the solar rays can be estimated by:

$$I_{br} = G_{sc} P^M \quad (3)$$

$$M = \frac{1}{\sin \alpha} \quad (4)$$

where  $P$  is the atmospheric transparency factor and  $M$  is the air mass and is calculated from the relationship with the altitude angle [40]. This value has certain variations; for this reason, the value of the distance between the sun and the earth is considered extraterrestrial radiation  $G_{ex}$ .

$$G_{ex} = G_{sc} \left( \frac{R_{av}}{R} \right)^2 \quad (5)$$

where  $R_{av}$  is the mean distance between the Sun and the Earth and  $R$  the instantaneous distance between the Sun and the Earth; this value depends on the day of the year or day number ( $N$ ). An approximation is given by:

$$\left( \frac{R_{av}}{R} \right) = 1 + 0.034 \left( \frac{2\pi N}{365} \right) \quad (6)$$

Considering extraterrestrial solar radiation, the unit of time incident to the right on the square meter of a surface results in:

$$G_{ex} = G_{sc} \left( 1 + 0.034 \cos \left( \frac{2\pi N}{365} \right) \right) \quad (7)$$

However, when direct radiation is considered in a horizontal plane with a tilted plane, it can be calculated considering Equation (3) [40]:

$$I_{bH} = I_{br} \sin \alpha \quad (8)$$

$$I_{b\beta} = I_{br}(\sin \alpha \cos \beta + \cos \alpha \cos \theta_s \sin \beta) \quad (9)$$

If the surface is not normal to the Sun, the solar radiation falling on it will be reduced by the cosine of the angle between the surface normal and a central sun ray. Figure 2 depicts the direct solar irradiance on a surface ( $I_o$ ), considering the angle between the surface's normal vector and a central solar ray (zenith angle)  $\theta_z$ . It becomes evident that when the surface area A surpasses its projected area (represented as hypothetical surface B), this results in a diminished solar energy flux per unit area on surface A in comparison to surface B.

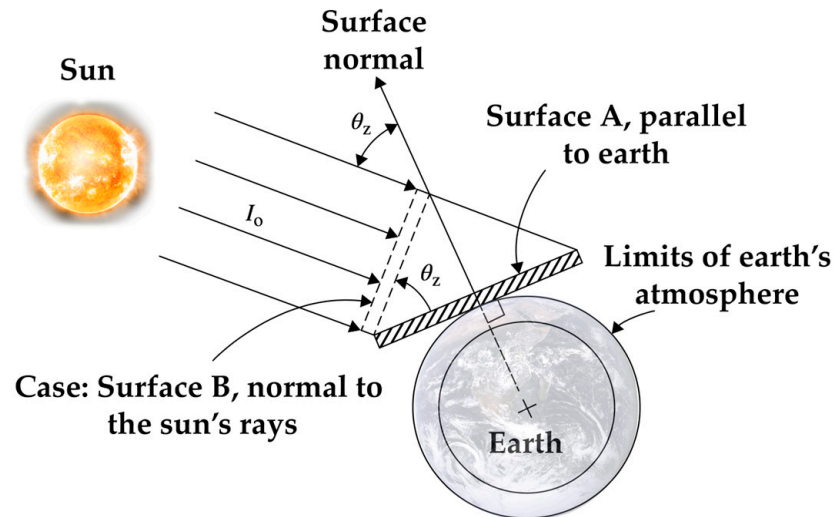


Figure 2. Extraterrestrial solar radiation on a horizontal surface.

Consequently, the extraterrestrial solar radiation on a horizontal surface located at a specific location  $G_{exH}$ .

$$G_{exH} = G_{ex} \cos \varphi \quad (10)$$

where  $\varphi$  is the solar zenith angle, which is measured from directly overhead to the geometric center of the Sun's disc. The solar zenith angle value is equal to the altitude value.

$$G_{exH} = G_{sc} \left( 1 + 0.034 \cos \left( \frac{360N}{365} \right) \right) \sin \mathcal{L} \sin \delta + \cos \mathcal{L} \cos \delta \cos \omega \quad (11)$$

Thus, the total extraterrestrial solar energy  $E_{ex}$  in  $W/m^2$  units is given by:

$$E_{ex} = \int_{T_{sr}}^{T_{ss}} G_{exH} dt \quad (12)$$

The extraterrestrial solar radiation on a tilted surface for a day ( $E_s$ ) can be calculated [39]:

$$E_s = \frac{24.36}{2\pi} \int_{\omega_s}^{\omega_r} G_{sc} \left( 1 + 0.034 \cos \left( \frac{360N}{365} \right) \right) \cos \theta d\omega \quad (13)$$

$$\begin{aligned} \cos \theta = & \sin \delta \sin \mathcal{L} \cos \beta - \sin \delta \cos \mathcal{L} \sin \beta \cos \theta_s \\ & + \cos \delta \cos \mathcal{L} \cos \beta \cos \omega + \cos \delta \sin \mathcal{L} \sin \beta \cos \theta_s \cos \omega \\ & + \cos \delta \sin \beta \sin \theta_s \sin \omega \end{aligned} \quad (14)$$

where  $\omega_r$  and  $\omega_s$  represents the hour of sunrise and the hour of sunset.

### 2.3. Extraterrestrial Solar Radiation Profile in a Residential House with an Isolated Photovoltaic System

The localization and design of the residential photovoltaic system (PV) were conducted using OpenSolar software version 2.14.01. Within the designated area, monocrystalline solar panels were selected over polycrystalline ones owing to their demonstrated increase in efficiency concerning solar radiation energy levels [41]. Figure 3 depicts the residential location along with the placement of the solar panel array, which is oriented towards the south.



**Figure 3.** Location of the photovoltaic system (in the red box) for the house.

In consideration of the residential house's geographical coordinates, latitude 19.6977 and longitude  $-103.4528$ , we determined the altitude and azimuth angles, which measured  $70.9562^\circ$  and  $75.8529^\circ$ , respectively. Utilizing the equations outlined in Section 2.2 for analyzing extraterrestrial solar radiation, we computed the received solar radiation during the summer season. The anticipated optimal extraterrestrial solar radiation profile attains an approximate value of  $1300 \text{ W/m}^2$  at solar noon. Figure 4 provides a visual representation of the solar radiation patterns observed on the surface of the implemented system.

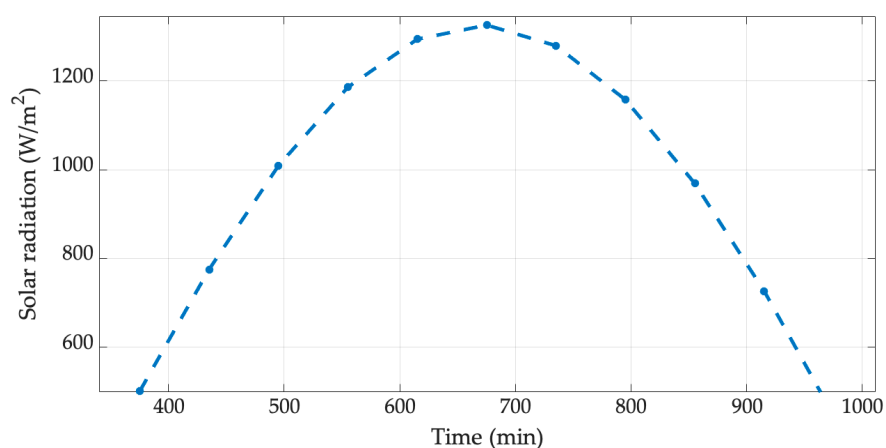


**Figure 4.** Daily extraterrestrial solar radiation for the houses with isolated photovoltaic systems.

### 2.4. PV Power Analysis and Installation

The isolated photovoltaic system is interconnected to a maximum power point tracking (MPPT) controller, a frequency converter (DC/AC 60 Hz), a storage battery, and fluorescence lamps as a load. The conversion of solar irradiance into solar energy occurs through the photovoltaic (PV) array. The resultant solar energy is employed for appliance operation

or stored within the battery. In instances where there is insufficient solar energy available, the battery provides the necessary energy to operate the appliances. Figure 5 shows the complete scheme of the installation of the PV system and its application of luminaires.

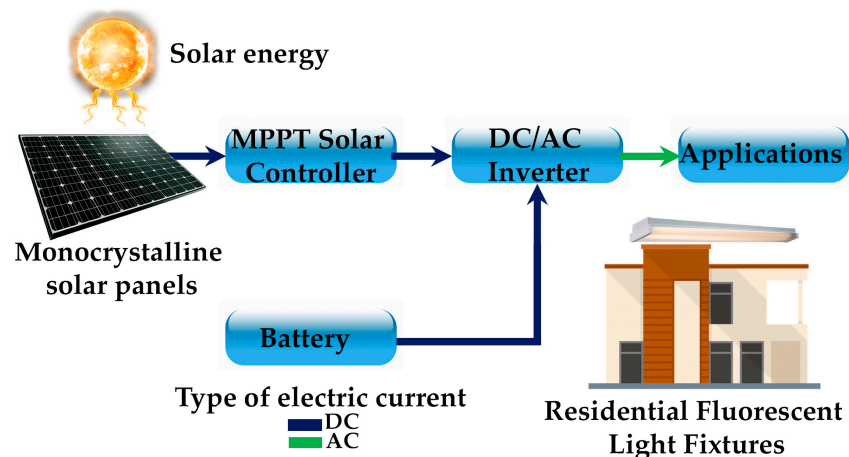


Figure 5. Residential off-grid energy system.

The photovoltaic panels are standard general-purpose technology, and according to the technical specification located on the panel's back side, they have the following parameters in Table 1.

Table 1. PV array specifications.

Parameter	Value
Maximum nominal power ( $P_{max}$ )	314 W
Open circuit voltage ( $V_{oc}$ )	47.16 VDC
Maximum voltage of power ( $V_{mp}$ )	39.41 VDC
Short circuit current ( $I_{sc}$ )	8.41 Amp
Maximum current of power ( $I_{mp}$ )	7.97 Amp
Nominal Operative Temperature Cell (NOTC)	Irradiance 800 W/m <sup>2</sup> , Environmental temperature 20 °C, Wind Velocity 1 m/s

The type of battery used for the installation is a standard lead-acid car battery model BCI EN-34/78-750, due to its low cost, high performance, and easily replaceable materials. This type of device is recommended for laboratory design to develop open-source designs for research purposes. Additionally, these materials adhere to current recycling protocols as they can be reused. Table 2 shows the most important characteristics of this type of battery.

Table 2. Battery specifications.

Parameter	Value
Voltage	12 VDC
Starting capacity (AC)	937 Amp
Cold Cranking Capacity (CCA)	750 Amp
BCI	34/78
Wet Weight (kg)	18.371 kg

The second stage is a low-capacity general-purpose MPPT controller, and according to the manufacturing trademark, the parameters are as follows in Table 3:

**Table 3.** MPPT controller parameters.

Parameter	Value
Nominal system voltage	12/24 VDC auto
Nominal charge current	30 Amp
Nominal discharge current	30 Amp
Battery voltage range	8–32 VDC
Open circuit maximum voltage cell	100 VDC
MPPT range voltage	2–72 VDC
Maximum voltage of power on the cell	390 W/12 VDC 780 W/24 VDC

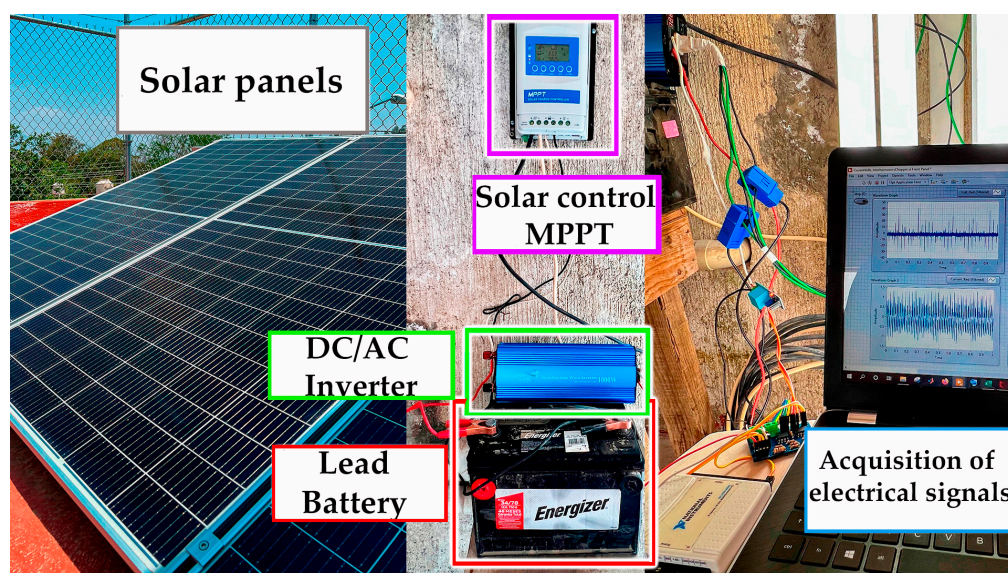
The third stage is the DC/AC conversion to 60 Hz, 120 alternating current voltage (VAC), resulting in a sinusoidal signal with a 1000 W maximum. The cell-generated energy is stored on an acid-plumb battery, and the MPPT connects the output converter to a series of fluorescence lamps with a minor to 1000 watts between 1 and 2 Amp consumption. Figure 6 shows the photovoltaic cells with 2 serial modules, the controller-converter-storage stage and data acquisition system, and voltage and current AC sensors. The generation of PV energy is influenced by panel efficiency, received solar radiation, and other factors. The energy at the system output is calculated using the following equations:

$$P_{max}(t, m) = FF \cdot V_{oc}(t, m) \cdot I_{sc}(t, m) \cdot N \quad (15)$$

where  $P_{max}$  is the maximum PV system power output,  $t$  represents the time (hours),  $m$  is the month of the year,  $FF$  is the fill factor, and  $N$  is the number of PV modules forming the PV system.

$$FF = \frac{V_{mp} \cdot I_{mp}}{V_{oc} \cdot I_{sc}} \quad (16)$$

where  $V_{mp}$  is the PV module voltage at the maximum power point (VDC) and  $I_{mp}$  is the current of the PV module at the maximum power point (Amp).

**Figure 6.** Photovoltaic system mounted in a residential house.

### 2.5. Signal Acquisition and Processing

The acquisition of electrical signals from the inverter output was performed using alternating current sensors, which were interconnected with arrays of fluorescent lamps located in various positions within the residential house. ZMPT101B voltage sensors were used to measure the RMS AC voltage generated, and SCT-013-100 sensors were

used to measure the RMS AC current. A NI-DAQ-6009 data acquisition card was used in conjunction with LabVIEW 2021 software, with a sampling rate of 10.504 kHz. The computational program was set up with the necessary calculations to estimate the inverter output energy. Antialiasing filters were also employed to obtain accurate measurements. Figure 7 demonstrates the required conditioning circuit for the current sensor and the measurement reading using the DAQ with A/D conversion.

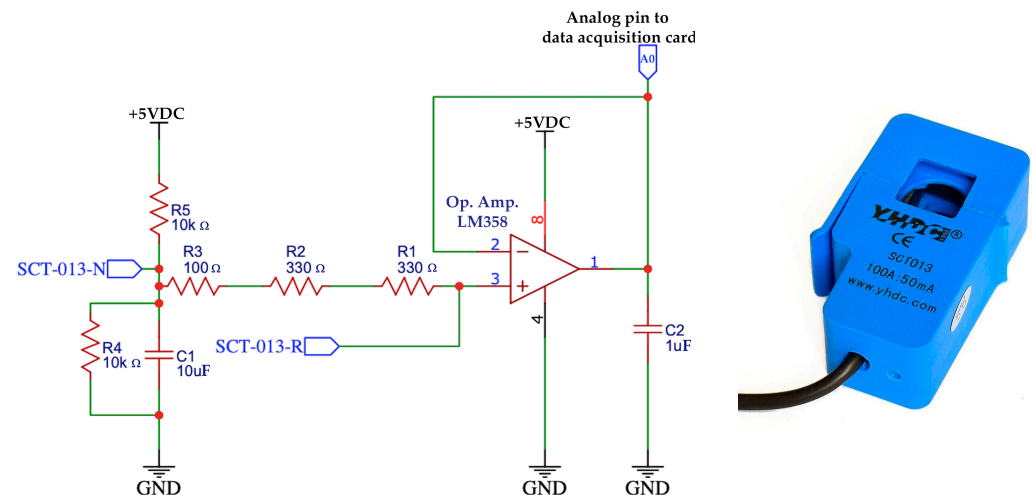


**Figure 7.** Signal conditioning circuit and AC current sensor.

The processing of electrical signals involves transforming the signals from the time domain to the frequency domain. The algorithm was executed after obtaining the AC and voltage electrical signals using Matlab™ 2019 software. The Wavelet Synchrosqueezed Transform (SSWT) was applied due to its superior characteristics in analyzing electrical signals in power grids and achieving visualization of harmonic/interharmonic frequencies with spectrograms. The use of this method can be found in studies related to interharmonic analysis [27]. Figure 8 summarizes the electrical signal processing stage.

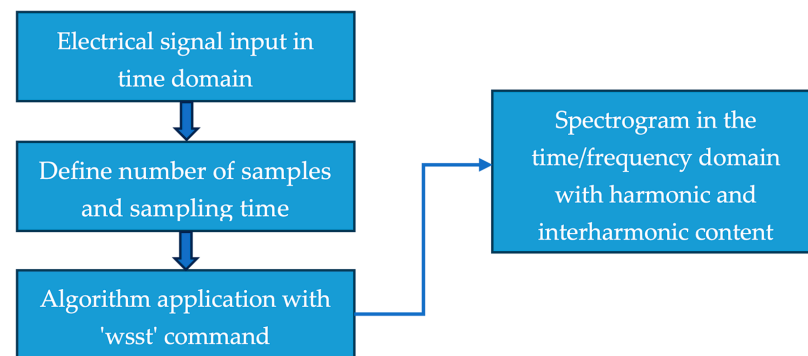


**Figure 8.** Electrical signal processing stage.

### 3. Case Studies and Results

This study was conducted in a residential setting housing a family of four, with fluorescent luminaires installed as linear loads in various living spaces within the residence. The selected season for examination was summer in the northern hemisphere, during which the maximum solar irradiance was calculated to reach 1300 W/m<sup>2</sup>. The average temperature ranged from 29 to 34 degrees Celsius (°C). The experiments were carried out on the same day, with measurements of electrical signals taken at 5 min intervals and fractions of seconds (0.2 s) for subsequent time-frequency analysis using spectrograms. The experimental conditions encompassed the following scenarios:

1. Optimal conditions: Temperature and solar radiation levels were at their peak at noon.
2. Partial conditions: Temperature and solar radiation levels decreased after dawn.
3. Nearly zero conditions: Temperature and solar radiation levels were minimal near sunset.
4. Absence of conditions: There was no temperature or solar radiation during the nighttime.

### 3.1. Case 1: Optimal Conditions of Temperature and Solar Radiation

In the first case, we conducted an analysis of the energy efficiency of luminaires installed in a family residence under Standard Test Conditions (STC) for the solar panels. The solar irradiance was calculated at the point of maximum power and recorded at levels ranging from 1150 to 1279 W/m<sup>2</sup>. These measurements were taken during a specific period, precisely at midday when solar energy and natural light were at their peak, with an average temperature of 32 °C. The MPPT solar controller was configured for standard operation, and we found that the harmonic generation performance at the output of the sinusoidal DC/AC inverter exhibited no significant voltage fluctuations or distortions.

Figure 9 provides an illustration of the generation of fundamental harmonics and odd harmonics, all with values below 8 VAC. Despite the presence of interharmonic oscillations in the current, the operation of the interconnected luminaires located in various areas of the building remained optimal. There were no visible or perceivable changes in the luminous intensity of the luminaires.

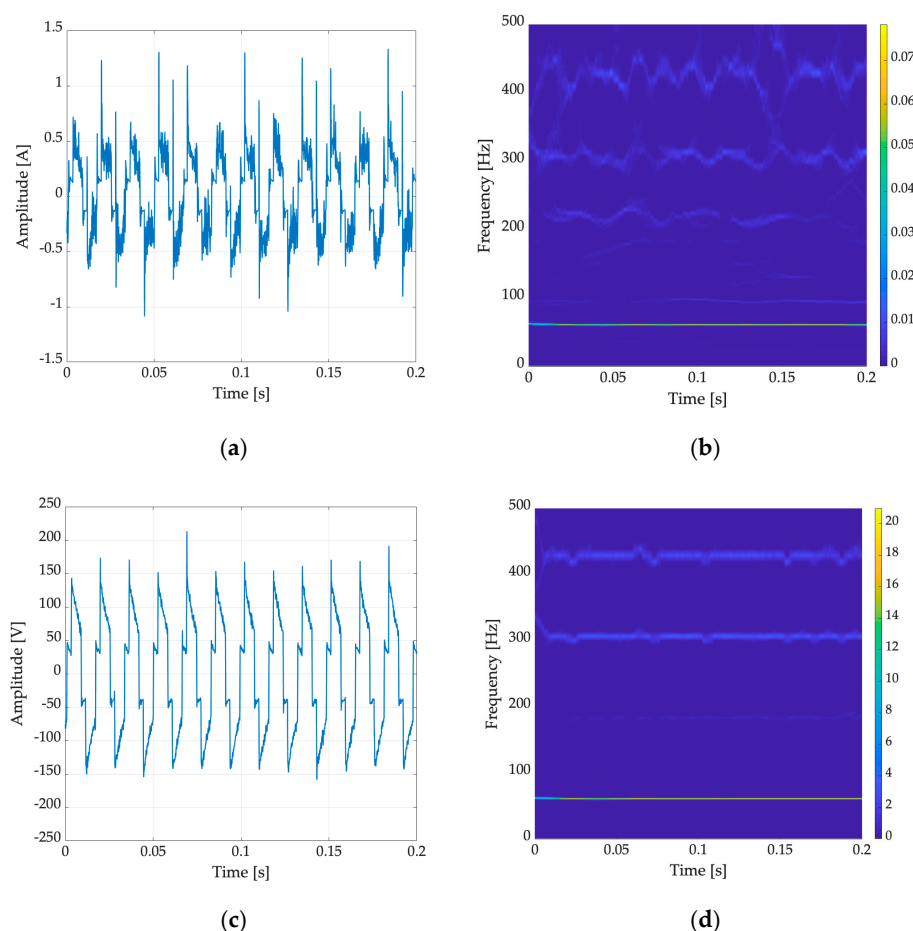


**Figure 9.** Output voltage and current signals in the DC/AC converter inverter of the photovoltaic system in optimal radiance conditions. (a) Electrical nominal current signal from luminaires; (b) Spectrogram of nominal current with harmonic and interharmonic content; (c) Electrical nominal voltage signal from output inverter; (d) Spectrogram of nominal voltage with harmonic content.

Further analysis through spectrograms revealed that the most significant interharmonics appeared at frequencies of 95.85 Hz, 225 Hz, and 313.6 Hz. It is important to note that these values did not have a significant short-term impact on the luminaires' performance. However, it is essential to consider the medium- and long-term implications, especially when luminaires with energy storage capabilities are in use. In such cases, the photovoltaic installation devices could experience overheating, potentially leading to decreased performance of the residence's luminaires. This is especially critical when the solar controller requires continuous operation throughout the day, considering various scenarios with varying levels of solar irradiance and temperature.

### 3.2. Case 2: Partial Conditions of Temperature and Solar Radiation

In the second scenario, we assessed the performance of half of the photovoltaic system operating at only half of its designed efficiency. This configuration was achieved by shading 50% of the cells in the solar panel array, resulting in reduced solar radiance levels falling below  $800 \text{ W/m}^2$ . Despite experiencing relatively high temperatures, averaging around  $34 \text{ }^\circ\text{C}$  during the summer season, we observed a significant interharmonic generation effect when the panels were not optimally positioned.

Under these conditions of partial sunlight exposure on the cells in the panels, noteworthy interharmonics emerged around the current harmonics, as evident in the spectrogram displayed in Figure 10a, with peaks at 179.3 Hz, 183.3 Hz, and 191.7 Hz. Additionally, a third harmonic of voltage was observed, as depicted in the spectrogram of Figure 10b.

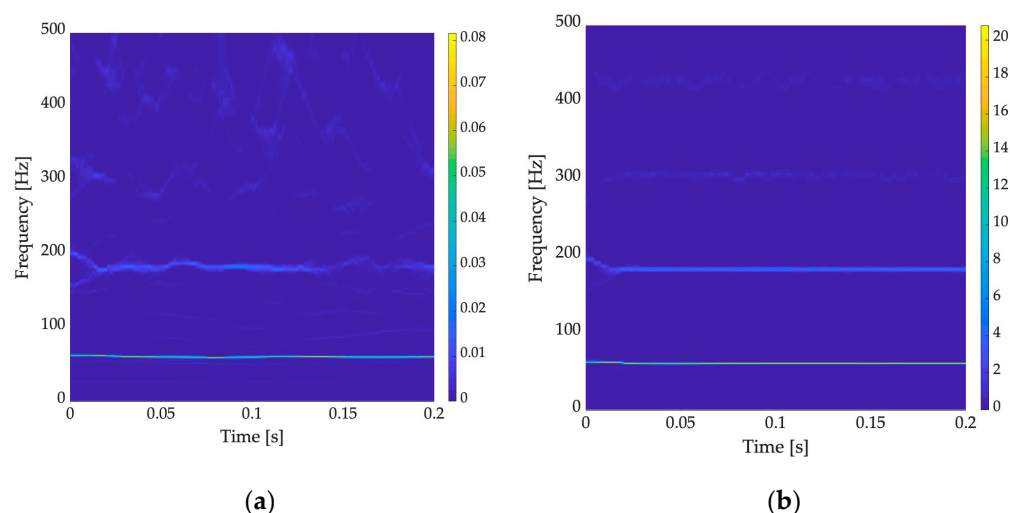


**Figure 10.** Spectrogram of output voltage and current signals in the DC/AC converter inverter of the photovoltaic system under partial radiance conditions. (a) Spectrogram of nominal current with significant interharmonic content. (b) Spectrogram of nominal voltage with odd harmonics.

This observation bears significance for luminaires, as it indicates a heightened consumption of stored energy during the day, ultimately leading to decreased performance with a reduced energy reserve available for nighttime use. Furthermore, if additional fluorescent lamp sequences were to be implemented in various areas of the residence, the overall energy consumption would increase, potentially necessitating restrictions on their usage.

### 3.3. Case 3: Almost Zero Conditions of Temperature and Solar Radiation

In the third case, we examined a scenario characterized by an almost complete under-utilization of sunlight, with a notable 70% absence of solar radiation ( $250 \text{ W/m}^2$ ) and a decreasing temperature that dropped to below  $22 \text{ }^\circ\text{C}$ . During the operation of the photovoltaic system, we observed evident oscillations and fluctuations in the electrical signals of

the luminaires, leading to variations in their luminous intensity. The root cause of these fluctuations lies in the interharmonics generated within the waveforms.

Given that this is a 120 VAC/60 Hz system, we noted voltage variations of up to 200 VAC during system startup. These variations are not only detrimental but also pose a potential hazard, affecting not only the interconnected lighting system within the living spaces but also the overall performance and functionality of the photovoltaic system when it is active. This impact is particularly pronounced on the solar controller and the voltage inverter, both of which comprise multiple electronic components.

Figure 11 visually illustrates the current distortions and voltage fluctuations, revealing clusters of harmful interharmonics, notably in proximity to the first and third harmonics, situated at 122.6 Hz and 175.3 Hz, respectively. These interharmonics exhibited significant magnitudes, ranging between 6 and 10 volts. Under these varying voltage conditions, the luminaires experienced flickering, leading to a negative phenomenon known as the Flicker effect [29,30]. This effect is caused by the generation of interharmonics and substantial voltage fluctuations over time. Furthermore, the generated current contained interharmonics with magnitudes ranging from 0.01 to 0.04 amperes, which had a discernible impact on the optimization of the MPPT solar controller [25,28].

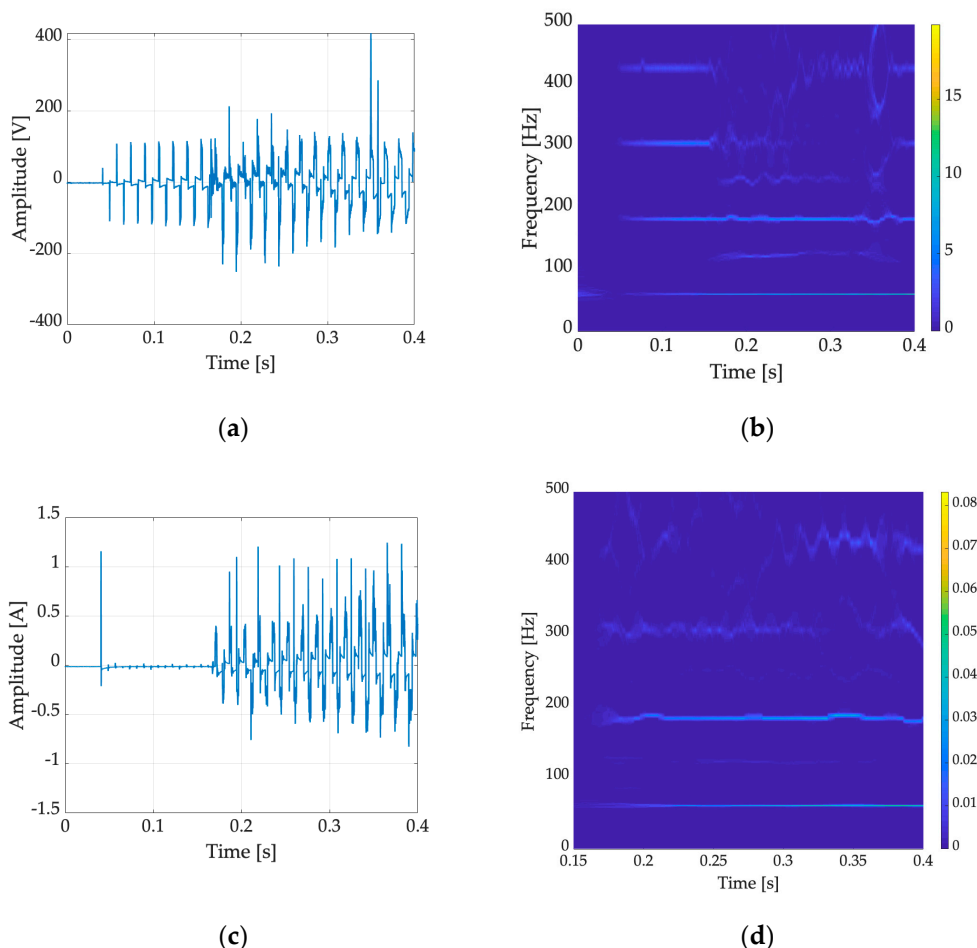


**Figure 11.** Spectrogram of output voltage and current signals in the DC/AC converter inverter of the photovoltaic system under almost zero radiance conditions. (a) Electrical nominal voltage signal from luminaires with fluctuations; (b) Spectrogram of nominal voltage with dangerous harmonic and interharmonic content; (c) Electrical nominal current signal from luminaires; (d) Spectrogram of nominal voltage with interharmonic content.

### 3.4. Case 4: Absence of Temperature and Solar Radiation

In the absence of sunlight and irradiance, particularly during the night, power generation relies solely on the voltage stored in the battery, derived from the solar panels. In the corresponding spectrograms presented in Figure 12a,b, a similar pattern of behavior was demonstrated when the photovoltaic (PV) system generated power during the daytime under optimal environmental conditions. During this nighttime operation, there were negligible current interharmonics observed at frequencies of 149.9 Hz, 183.3 Hz, and 293.3 Hz.

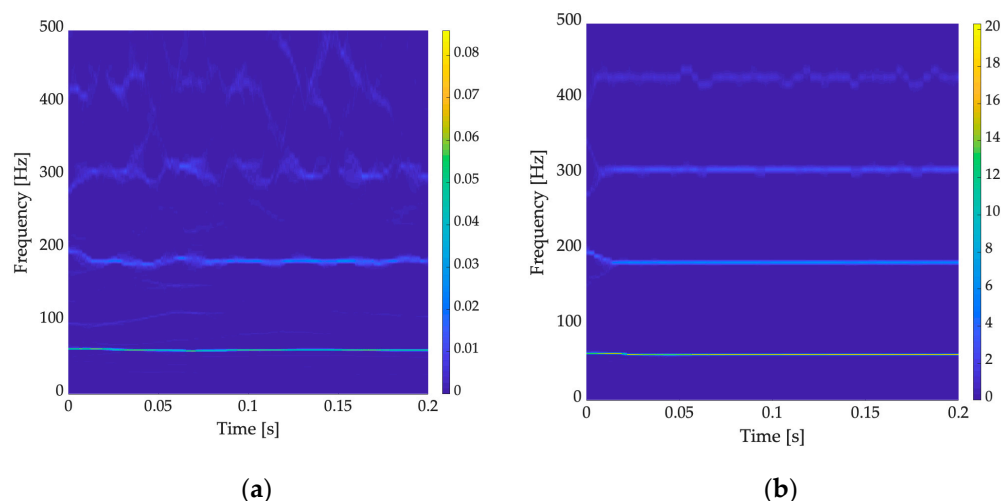


**Figure 12.** Spectrogram of output voltage and current signals in the DC/AC converter inverter of the photovoltaic system under the absence of radiance conditions. (a) Spectrogram of nominal current with odd harmonics and interharmonic content. (b) Spectrogram of nominal voltage with odd harmonics.

This process is intrinsically tied to the energy generated by the solar panels during daylight hours, which is then stored for later use. However, it is essential to note that if the protective measures or adjustments to account for solar radiation, particularly in standard test conditions (STC) or NOTC (Night Operation Test Conditions) operations of the PV system, are not properly installed, taking into consideration the azimuth angle, the effective utilization of sunlight during the day can be compromised.

Table 4 provides a comprehensive summary of the examined cases, including the outcomes obtained, the environmental conditions surrounding the solar system (comprising calculated irradiance levels), and the noteworthy interharmonic current generation observed within the living spaces.

**Table 4.** Summary results of different case studies of environmental conditions for interharmonic generation.

Case Studies	Storage Energy on Battery (Volt/Amp)	The Most Significant Interharmonic (Hz/Amp)	Extraterrestrial Solar Radiation (W/m <sup>2</sup> )
1	14.3/8.3	95.85/0.03	1200
2	13.1/3.6	183.3/0.037	600
3	12.5/2.9	187.5/0.04	250
4	12/1.7	149.9/0.01	0

It is crucial to emphasize that the impact of solar radiation received, which is contingent on the position and location of the photovoltaic system, has a direct influence on energy efficiency. This influence is attributed to the presence of harmonic and interharmonic components, which not only affect the performance of the luminaires but also

have ramifications for the overall efficiency of the photovoltaic inverter and the MPPT solar controller.

#### 4. Discussion

This research delves into the utilization of solar energy in isolated energy storage systems, with a particular focus on lighting applications within residential spaces, providing a comprehensive insight into a critical facet of zero-energy buildings. The phenomenon of interharmonic generation in such isolated photovoltaic systems warrants thorough consideration due to its intricate interplay with solar panel performance and the effective harnessing of daylight [19]. The results obtained in this research shed light on the influence of environmental conditions and solar radiation on the performance of luminaires installed in a residential setting. The experiments were conducted in different scenarios simulating everyday situations, and the findings reveal valuable information about the energy efficiency and behavior of photovoltaic systems interconnected with luminaires.

Solar irradiance at the maximum power point remained at elevated levels, and no significant fluctuations were detected in the generation of harmonics at the output of the sinusoidal DC/AC inverter. While interharmonics were identified in the currents, they did not have a visible impact on the luminous intensity of the luminaires.

However, it is important to highlight the presence of significant interharmonics at specific frequencies, such as 95.85 Hz, 225 Hz, and 313.6 Hz. Notably, as solar energy utilization percentages decrease, the propensity for heightened interharmonic generation becomes more pronounced, especially under conditions of reduced irradiance and temperature [23–25,28]. Although an immediate impact on luminaire performance was not observed, it is essential to consider the medium- and long-term implications, especially when luminaires with energy storage capacity are utilized. In such cases, photovoltaic installation devices could risk overheating, potentially leading to reduced performance of the residence's luminaires.

The presence of high levels of harmonics and interharmonics has several consequences for luminaries and the residential photovoltaic system, especially incandescent lamps with fast variations in AC voltage. In the context of advancing zero-energy building paradigms, the implementation of adaptive control strategies within MPPT controllers assumes significant utility [25,28]. Such strategies prove invaluable in responding to variations in irradiance, which have the potential to influence the performance of DC energy generation by solar panels. These adaptive control mechanisms contribute to the fine-tuning of energy production processes and help maintain stability in energy output [34–36].

In the second scenario, when evaluating the performance of the photovoltaic system under partial conditions, significant interharmonics related to the partial exposure of solar cells to sunlight were observed. These interharmonics affected the consumption of stored energy during the day, which could result in reduced performance during the night. Furthermore, if additional sequences of fluorescent lamps were added in different areas of the residence, the total energy consumption would increase, potentially necessitating usage restrictions.

In the third scenario, characterized by a nearly complete lack of solar utilization, clear oscillations and fluctuations were observed in the electrical signals of the luminaires. These fluctuations had a significant negative impact on the photovoltaic system and the MPPT solar controller. The interharmonics generated during this operation also contributed to the flickering effect of the luminaires.

It is important to note that, during nighttime operation, energy generation relies solely on the voltage stored in the battery, derived from the solar panels. This underscores the importance of implementing appropriate protective measures and adjustments to ensure the effective utilization of solar energy during the day. The orientation, panel positioning, and solar radiation have a significant impact on the lighting appliances in residential houses

and energy production. Therefore, it is important to consider external factors that can influence energy efficiency, such as climate conditions [35].

In summary, the results of this research underscore the relevance of environmental conditions and solar radiation to the energy efficiency of photovoltaic systems interconnected with luminaires. The presence of harmonics and interharmonics affects both luminaire performance and the overall efficiency of the photovoltaic inverter and MPPT solar controller [22,25]. These findings have significant implications for the design and management of photovoltaic systems in residential environments and could be valuable for optimizing the performance and reliability of such systems under various climatic and solar radiation conditions.

## 5. Conclusions

The utilization of solar energy in zero-energy buildings, particularly in residential spaces equipped with lighting fixtures and appliances, must be approached with care and precision [3,15]. Our research has highlighted the critical relationship between environmental conditions, specifically solar radiation received in photovoltaic-based energy storage systems, and its potential impact on building luminous intensity due to electrical disturbances caused by harmonics and interharmonics [24,31,33]. Notably, extraterrestrial solar radiation below  $300 \text{ W/m}^2$  has adverse effects on luminaires, especially when the lighting system is in operation, resulting in detrimental levels of current and voltage interharmonics, unlike the optimal operating conditions during daylight hours.

In alignment with SDG-7 and its focus on clean energy infrastructure, carbon dioxide emissions reduction, and the enhancement of residential applications within building design, it is evident that these objectives are intricately linked to the energy efficiency of photovoltaic systems, the interconnection of electronic equipment, and the effectiveness of devices such as controllers and batteries [20].

Architectural photovoltaic applications (APAs) should prioritize the seamless integration of photovoltaics into design and installation conditions to ensure efficient energy utilization when sunlight is available for most of the day. Our research has demonstrated that different solar radiation conditions, as well as total or partial shading of solar modules, lead to increased generation of unwanted interharmonic contents, subsequently affecting the performance of installed luminaires. Additionally, these variations are dependent on factors such as the positioning of the photovoltaic system, its azimuth angle, and its altitude [35].

While our experiments were limited to a single residential space, it is clear that future research endeavors should focus on luminaire applications in residential settings under the influence of diverse radiation conditions and location-specific effects within photovoltaic systems, whether they are based on energy storage or isolated from the electrical network. Expanding our understanding of these complex interactions will be essential for advancing the design and implementation of solar-powered lighting systems in energy-efficient buildings.

**Author Contributions:** Conceptualization, J.J.-C. and F.C.F.; methodology, J.J.-C.; software, A.G.-O. and S.S.P.; validation, J.J.-C., J.C.-C. and F.C.F.; formal analysis, J.J.-C. and A.G.-O.; investigation, F.C.F., J.C.-C. and J.J.-C.; resources, J.J.-C.; data curation, S.S.P. and A.G.-O.; writing—original draft preparation, J.J.-C., F.C.F., S.S.P. and A.G.-O.; writing—review and editing, J.C.-C. and F.C.F.; visualization, A.G.-O.; supervision, J.J.-C.; project administration, F.C.F.; funding acquisition, J.C.-C., J.J.-C. and F.C.F. All authors have read and agreed to the published version of this manuscript.

**Funding:** This research was funded by UPV (Ministry of Universities, Recovery, Transformation, and Resilience Plan—Funded by the European Union—Next Generation EU) and Postdoctoral Research (PAIDPD-22).

**Data Availability Statement:** The data presented in this study are available on request from the corresponding author.

**Acknowledgments:** The authors acknowledge the full financial support for this research provided by María Zambrano (UPV, Ministry of Universities, Recovery, Transformation, and Resilience Plan—Funded by the European Union—Next Generation EU) of the Institute of Materials Technology of the Polytechnic University of Valencia (Spain) and UPVs Aid to Promote Postdoctoral Research (PAIDPD-22).

**Conflicts of Interest:** The authors declare no conflict of interest. The funders had no role in the study's design, in the collection, analyses, or interpretation of data, in the writing of the manuscript, or in the decision to publish the results.

## References

1. Gu, D.; Andreev, K.; Dupre, M.E. Major Trends in Population Growth around the World. *China CDC Wkly.* **2021**, *3*, 604–613. [[CrossRef](#)] [[PubMed](#)]
2. Arora, N.K.; Mishra, I. United Nations Sustainable Development Goals 2030 and environmental sustainability: Race against time. *Environ. Sustain.* **2019**, *2*, 339–342. [[CrossRef](#)]
3. Li, X.; Lin, A.; Young, C.-H.; Dai, Y.; Wang, C.-H. Energetic and economic evaluation of hybrid solar energy systems in a residential net-zero energy building. *Appl. Energy* **2019**, *254*, 113709. [[CrossRef](#)]
4. Kuwahara, R.; Kim, H.; Sato, H. Evaluation of Zero-Energy Building and Use of Renewable Energy in Renovated Buildings: A Case Study in Japan. *Buildings* **2022**, *12*, 561. [[CrossRef](#)]
5. Sarker, S.A.; Wang, S.; Adnan, K.M.M.; Anser, M.K.; Ayoub, Z.; Ho, T.H.; Tama, R.A.Z.; Trunina, A.; Hoque, M.M. Economic viability and so-cio-environmental impacts of solar home systems for off-grid rural electrification in Bangladesh. *Energies* **2020**, *13*, 679. [[CrossRef](#)]
6. Lee, H.; Han, S.; Seo, J. Light Shelf Development Using Folding Technology and Photovoltaic Modules to Increase Energy Efficiency in Building. *Buildings* **2022**, *12*, 81. [[CrossRef](#)]
7. Kiwan, S.; Mosali, A.A.; Al-Ghasem, A. Smart Solar-Powered LED Outdoor Lighting System Based on the Energy Storage Level in Batteries. *Buildings* **2018**, *8*, 119. [[CrossRef](#)]
8. Kaliakatsos, D.; Nicoletti, F.; Paradisi, F.; Bevilacqua, P.; Arcuri, N. Evaluation of Building Energy Savings Achievable with an Attached Bioclimatic Greenhouse: Parametric Analysis and Solar Gain Control Techniques. *Buildings* **2022**, *12*, 2186. [[CrossRef](#)]
9. Pokorny, N.; Matuska, T. Glazed photovoltaic-thermal (PVT) collectors for domestic hot water preparation in multifamily building. *Sustainability* **2020**, *12*, 6071. [[CrossRef](#)]
10. Eshraghi, J.; Narjabadifam, N.; Mirkhani, N.; Khosroshahi, S.S.; Ashjaee, M. A comprehensive feasibility study of applying solar energy to design a zero energy building for a typical home in Tehran. *Energy Build.* **2014**, *72*, 329–339. [[CrossRef](#)]
11. Li, D.H.W.; Aghimien, E.I.; Alshaibani, K. An Analysis of Real-Time Measured Solar Radiation and Daylight and Its Energy Implications for Semi-Transparent Building-Integrated Photovoltaic Façades. *Buildings* **2023**, *13*, 386. [[CrossRef](#)]
12. Vanaga, R.; Blumberga, A.; Freimanis, R.; Mols, T.; Blumberga, D. Solar facade module for nearly zero energy building. In Proceedings of the 3rd International Conference on Smart Energy Systems and 4th Generation District Heating (SES4DH), Copenhagen, Denmark, 12–13 September 2017; pp. 1025–1034.
13. Bhargawa, A.; Singh, A.K. Solar Irradiance, Climatic Indicators, and Climate Change—An Empirical Analysis. *Adv. Space Res.* **2019**, *64*, 271–277. [[CrossRef](#)]
14. Haghighi, Z.; Dehnavi, M.A.; Konstantinou, T.; Van Den Dobbelen, A.; Klein, T. Architectural photovoltaic applications: Lessons learned and perceptions from architects. *Buildings* **2021**, *11*, 62. [[CrossRef](#)]
15. Naranjo-Mendoza, C.; Oyinlola, M.A.; Wright, A.J.; Greenough, R.M. Experimental study of a domestic solar-assisted ground source heat pump with seasonal underground thermal energy storage through shallow boreholes. *Appl. Therm. Eng.* **2019**, *162*, 114218. [[CrossRef](#)]
16. Maghrabie, H.M.; Abdelkareem, M.A.; Al-Alami, A.H.; Ramadan, M.; Mushtaha, E.; Wilberforce, T.; Olabi, A.G. State-of-the-Art Technologies for Building-Integrated Photovoltaic Systems. *Buildings* **2021**, *11*, 383. [[CrossRef](#)]
17. Michalak, P. Modelling of Solar Irradiance Incident on Building Envelopes in Polish Climatic Conditions: The Impact on Energy Performance Indicators of Residential Buildings. *Energies* **2021**, *14*, 4371. [[CrossRef](#)]
18. Cho, D.; Valenzuela, J. Optimization of residential off-grid PV-battery systems. *Sol. Energy* **2020**, *208*, 766–777. [[CrossRef](#)]
19. Karaca, A.E.; Dincer, I. A new integrated solar energy based system for residential houses. *Energy Convers. Manag.* **2020**, *221*, 113112. [[CrossRef](#)]
20. Li, H.; Song, Y.; Zhu, M.; Jiao, Y. Experimental Interharmonic Sensitivity Evaluation of LED Lamps Based on the Luminous Flux Flicker Model. *Energies* **2022**, *15*, 2990. [[CrossRef](#)]
21. Drapela, J.; Halpin, M.; Langella, R.; Meyer, J.; Mueller, D.; Sharma, H.; Testam, A.; Watson, N.R.; Zech, D. Issues and challenges related to interharmonic distortion limits. In Proceedings of the 19th International Conference on Harmonics and Quality of Power (ICHQP), Dubai, United Arab Emirates, 6–7 July 2020; pp. 1–6.
22. Sangwongwanich, A.; Yang, Y.; Sera, D.; Blaabjerg, F. Mission profile-oriented control for reliability and lifetime of photovoltaic inverters. *IEEE Trans. Ind. Appl.* **2019**, *56*, 601–610. [[CrossRef](#)]
23. Ravindran, V.; Busatto, T.; Ronnberg, S.K.; Meyer, J.; Bollen, M.H.J. Time-Varying Interharmonics in Different Types of Grid-Tied PV Inverter Systems. *IEEE Trans. Power Deliv.* **2019**, *35*, 483–496. [[CrossRef](#)]

24. Elvira-Ortiz, D.A.; Morinigo-Sotelo, D.; Duque-Perez, O.; Osornio-Rios, R.A.; Romero-Troncoso, R.J. Study of the harmonic and interharmonic content in electrical signals from photovoltaic generation and their relationship with environmental factors. *J. Renew. Sustain. Energy* **2019**, *11*, 043502. [[CrossRef](#)]
25. Sangwongwanich, A.; Yang, Y.; Sera, D.; Soltani, H.; Blaabjerg, F. Analysis and Modeling of Interharmonics from Grid-Connected Photovoltaic Systems. *IEEE Trans. Power Electron.* **2018**, *33*, 8353–8364. [[CrossRef](#)]
26. Moradi, A.; Zare, F.; Kumar, D.; Sharma, R. The Influence of Background Voltage Interharmonics on Amplifying Current Distortions in Distribution Networks. In Proceedings of the IEEE International Conference on Power Electronics, Drives and Energy Systems (PEDES), Jaipur, India, 14–17 December 2022; pp. 1–6.
27. Gudiño-Ochoa, A.; Jalomo-Cuevas, J.; Molinar-Solís, J.E.; Ochoa-Ornelas, R. Analysis of Interharmonics Generation in Induction Motors Driven by Variable Frequency Drives and AC Choppers. *Energies* **2023**, *16*, 5538. [[CrossRef](#)]
28. Mao, M.; Xu, Z.; Li, J.; Li, H. A Phase-Shifting DC-Link Voltage Control Strategy for Parallel Inverters to Suppress Interharmonics in PV Systems. *IEEE J. Emerg. Sel. Top. Power Electron.* **2023**, *11*, 3163–3172. [[CrossRef](#)]
29. Drapela, J.; Langella, R.; Testa, A.; Grappè, J. A real life light flicker case-study with LED lamps. In Proceedings of the 18th International Conference on Harmonics and Quality of Power (ICHQP), Ljubljana, Slovenia, 13–16 May 2018; pp. 1–6.
30. Kim, T.; Rylander, M.; Powers, E.J.; Grady, W.M.; Arapostathis, A. LED Lamp Flicker Caused by Interharmonics. In Proceedings of the 2008 IEEE Instrumentation and Measurement Technology Conference, Victoria, BC, Canada, 12–15 May 2008; pp. 1920–1925.
31. Sandelic, M.; Sangwongwanich, A.; Blaabjerg, F. Impact of power converters and battery lifetime on economic profitability of residential photovoltaic systems. *IEEE Open J. Ind. Appl.* **2022**, *3*, 224–236. [[CrossRef](#)]
32. Kuang, W.Y.; Illankoon, C.; Vithanage, S.C. Grid-Connected Solar Photovoltaic (PV) System for Covered Linkways. *Buildings* **2022**, *12*, 2131. [[CrossRef](#)]
33. Sandelic, M.; Sangwongwanich, A.; Blaabjerg, F. Reliability Evaluation of PV Systems with Integrated Battery Energy Storage Systems: DC-Coupled and AC-Coupled Configurations. *Electronics* **2019**, *8*, 1059. [[CrossRef](#)]
34. Sandelic, M.; Sangwongwanich, A.; Blaabjerg, F. A systematic approach for lifetime evaluation of PV-battery systems. In Proceedings of the IECON 2019—45th Annual Conference of the IEEE Industrial Electronics Society, Lisbon, Portugal, 14–17 October 2019; Volume 1, pp. 2295–2300.
35. Bouguerra, S.; Yaiche, M.R.; Gassab, O.; Sangwongwanich, A.; Blaabjerg, F. The Impact of PV Panel Positioning and Degradation on the PV Inverter Lifetime and Reliability. *IEEE J. Emerg. Sel. Top. Power Electron.* **2020**, *9*, 3114–3126. [[CrossRef](#)]
36. Sangwongwanich, A.; Yang, Y.; Sera, D.; Blaabjerg, F. Lifetime evaluation of grid-connected PV inverters considering panel degradation rates and installation sites. *IEEE Trans. Power Electron.* **2017**, *33*, 1225–1236. [[CrossRef](#)]
37. Soulayman, S. Comments on solar azimuth angle. *Renew. Energy* **2018**, *123*, 294–300. [[CrossRef](#)]
38. Abood, A.A. A comprehensive solar angles simulation and calculation using matlab. *Int. J. Energy Environ.* **2015**, *6*, 367.
39. Widén, J.; Munkhammar, J. *Solar Radiation Theory*; Uppsala University: Uppsala, Sweden, 2019; ISBN 9789150627602.
40. Hao, D.; Qi, L.; Tairab, A.M.; Ahmed, A.; Azam, A.; Luo, D.; Pan, Y.; Zhang, Z.; Yan, J. Solar energy harvesting technologies for PV self-powered applications: A comprehensive review. *Renew. Energy* **2022**, *188*, 678–697. [[CrossRef](#)]
41. Kabulov, R.R.; Matchanov, N.A.; Umarov, B.R. Features of load current–voltage characteristics of a monocrystalline silicon solar cell at various levels of solar illumination. *Appl. Sol. Energy* **2017**, *53*, 297–298. [[CrossRef](#)]

**Disclaimer/Publisher’s Note:** The statements, opinions and data contained in all publications are solely those of the individual author(s) and contributor(s) and not of MDPI and/or the editor(s). MDPI and/or the editor(s) disclaim responsibility for any injury to people or property resulting from any ideas, methods, instructions or products referred to in the content.